Molecular Physics, Vol. 104, No. 18, 20 September 2006, 2901–2917

Taylor & Francis
Taylor & Francis Group

Zwanzig model of multi-component mixtures of biaxial particles: y^3 theory re-visited

E. P. SOKOLOVA*†, N. P. TUMANYAN†, A. YU. VLASOV† and A. J. MASTERS‡
†St. Petersburg State University, St. Petersburg, Russia
‡University of Manchester, Manchester, UK

(*Received 6 May 2006; accepted 19 June 2006*)

The paper considers the thermodynamic and phase ordering properties of a multi-component Zwanzig mixture of hard rectangular biaxial parallelepipeds. An equation of state (EOS) is derived based on an estimate of the number of arrangements of the particles on a three-dimensional cubic lattice. The methodology is a generalization of the Flory–DiMarzio counting scheme, but, unlike previous work, this treatment is thermodynamically consistent. The results are independent of the order in which particles are placed on the lattice. By taking the limit of zero lattice spacing, a translationally continuous variant of the model (the off-lattice variant) is obtained. The EOS is identical to that obtained previously by a wide variety of different approaches. In the off-lattice limit, it corresponds to a third-level y-expansion and, in the case of a binary mixture of square platelets, it also corresponds to the EOS obtained from fundamental measure theory. On the lattice it is identical to the EOS obtained by retaining only complete stars in the virial expansion. The off-lattice theory is used to study binary mixtures of rods ($R_1 - R_2$) and binary mixtures of platelets ($P_1 - P_2$). The particles were uniaxial, of length (thickness) L and width D. The aspect ratios $\Gamma_i = L_i/D_i$ of the components were kept constant ($\Gamma_{1R} = 15$, $\Gamma_{1P} = 1/15$ and $\Gamma_{2R} = 150$, $\Gamma_{2P} = 1/150$), so the second virial coefficient of R_1 was identical to P_1 and similarly for R_2 and P_2. The volume ratio of particles 1 and 2, v_1/v_2, was then varied, with the constraints that $v_{iR} = v_{iP}$ and $v_{2R} = 150D_{2R}^3$. Results on nematic–isotropic ($N - I$) phase coexistence at an infinite dilution of component 2, are qualitatively similar for rods and platelets. At small values of the ratio v_1/v_2, the addition of component 2 (i.e. a thin rod (e.g. a polymer) or a thin plate) results in the stabilization of the nematic phase. For larger values of v_1/v_2, however, this effect is reversed and the addition of component 2 destabilizes the nematic. For similar molecular volumes of the two components strong fractionation is observed: shorter rods and thicker platelets congregate in the isotropic phase. In general, the stabilization of the ordered phase and the fractionation between the phases are both weaker in the platelet mixtures. The calculated spinodal curves for isotropic-isotropic demixing are noticeably different between the $R_1 - R_2$ and the $P_1 - P_2$ systems. The platelet mixtures turn out to be stable with respect to de-mixing up to extremely high densities. The values of the consolute points for the $R_1 - R_2$ blends are remarkably similar to those obtained using the Parsons–Lee approximation for bi-disperse mixtures of freely rotating cylinders with similar aspect ratios [S. Varga. A. Galindo, G. Jackson, *Mol. Phys.*, **101,** 817 (2003)]. In a number of $R_1 - R_2$ mixtures, phase diagrams exhibiting both $N - I$ equilibrium and $I - I$ de-mixing were calculated. The latter is pre-empted by nematic ordering in all the cases studied. Calculations show the possible appearance of azeotropes in the $N - I$ coexistence domain.

1. Introduction

Much effort has gone into the study of the rich phase behaviour exhibited by liquid-crystal-forming colloidal suspensions. These systems are usually modelled in terms of mixtures of hard bodies of various shapes. Many of the theoretical approaches [1–4] are based on the ideas of Onsager [5], where the steric interactions are treated in terms of an orientational dependent second virial coefficient and all virial coefficients of higher order

*Corresponding author. Email: esok@evergreen.spb.ru

Molecular Physics
ISSN 0026–8976 print/ISSN 1362–3028 online © 2006 Taylor & Francis
http://www.tandf.co.uk/journals
DOI: 10.1080/00268970600867429

are neglected. While this methodology is exact for long, thin rods, it cannot quantitatively describe the phase behaviour of less anisotropic particles. Scaling methodologies [6] have provided an approximate but sometimes accurate means of extending the limits of applicability of Onsager's theory both to lower particle anisotropies and to higher fluid densities. Using these methods, a variety of interesting phenomena have been discovered, all resulting from the interplay between orientational and mixing entropic contributions and excluded volume effects. In the case of rod–rod [7, 8], rod–plate [8] and plate–plate [9] mixtures, such theories have predicted nematic–nematic and isotropic–isotropic de-mixing, the formation of biaxial phases and the fractionation of the longer rods and the thinner plates into the nematic phase. It is worth noting that theoretical predictions of such equilibria involving uniaxial nematic phases have been corroborated by experimental studies of sterically stabilized colloid rods [10] and of colloid platelets [11] dispersed in non-aqueous solvents.

An alternative theoretical strategy is to use models in which the particles can only take up discrete orientations. The off-lattice Zwanzig model [12] is of this type and has been extensively studied. The disadvantage with respect to Onsager-like theories is that not all orientations are allowed. The advantage is that one can readily go beyond second-virial level theories, incorporating higher virial coefficients, without the need for extensive numerical work. Qualitatively one would expect the predictions from the two types of theory to be similar. Examples of previous studies using the Zwanzig model are on the phase behaviour of binary mixtures of hard rectangular parallelepipeds (HRP) at the second and fourth levels of the virial equation [13], on biaxial nematic phase stability with respect to nematic–nematic phase separation in mixtures of rods and plates [14] and on fluid–fluid de-mixing in suspensions of long colloidal rods and stiff polymer in the limit of zero diameter [15].

Discrete orientation models are also interesting in their own right, as they form a convenient testing ground for density functional theories, such as Rosenfeld's fundamental measure theory (FMT) [16]. Cuesta [17] used such methods to study de-mixing in a binary mixture of parallel hard cubes, obtaining results in qualitative agreement with computer simulations. The approach was then extended by Martínez-Ratón and Cuesta to explore the possible transitions to inhomogeneous phases (such as smectic, columnar and plastic solid) and poly-dispersity effects in mixtures of rods and plates [18].

FMT was also applied to investigate the phase behaviour of inhomogeneous and bulk homogeneous binary mixtures of square platelets [19, 20]. The FMT free energy for the uniform phases turned out to be identical to a y variable expansion [21] carried out to third order (a y^3 theory). A nematic–nematic de-mixing transition was predicted for certain values of the model parameters and it was noted that the topology of the phase diagram was in agreement with results obtained for freely rotating platelets using the functional scaling approximation [9].

Another algorithm for calculating the properties of these discrete orientational models is to arrange the particles on a lattice and estimate the number of possible distinguishable arrangements. DiMarzio generalized the Flory–Huggins lattice arguments [22] to obtain a mean-field theory which described the isotropic-nematic transition in a system of hard rods [23]. Extensions to the theory have also been made so as to study the effects of side chain flexibility on the isotropic-nematic transition [24] and to investigate the nematic–smectic A transition [25].

In the case of mixtures, however, it has proved difficult to generalize this method in a way that is thermodynamically consistent. Shih and Alben [26] studied a system of biaxial rods with restricted orientations, but their estimate of the total number of configurations depended upon the order in which the objects were placed on the lattice. Later research by DiMarzio *et al*. [27] and by Boehm and Martire [28] on mixtures of hard rectangles on a square lattice suffers from the same difficulties. Study by Sokolova and Tumanyan [29] gives an enhanced counting scheme which, when applied to a case of multi-component mixtures of hard rectangles able of forming an orientationally ordered phase, provides thermodynamically consistent results.

However, the configurational partition function of a mixture of HRP*s* on a cubic lattice developed earlier by Tumanyan and Sokolova [30] has not been detailed so far. In this paper we first address this problem, so as to obtain thermodynamically consistent expressions for the Helmholtz energy of multi-component mixtures of bi-axial HRPs with restricted orientations. The excess free energy for the lattice model under study is identical to that obtained by retaining only the complete star diagrams in the virial expansion [36]. Furthermore, in the limit of zero lattice spacing the expression for the Helmholtz energy proved to be identical to the FMT and y^3 expansion expressions discussed earlier. The fact that these different theoretical approaches give the same answer is obviously no accident and might be of interest for further investigation.

The off-lattice version of the model has been applied to studies of orientational and thermodynamic properties of nematic systems modeling mixtures of

low-molecular mesogens [31, 32]. In this paper, we concentrate on bulk phase diagrams of mixtures composed of highly anisotropic in shape colloidal particles, making comparisons with previous theoretical work. Our results support the conclusion that this restricted orientation model can predict many aspects of phase behaviour as are found by studying continuous orientation models.

The paper is divided into four sections. The next section gives the thermodynamically consistent estimation of the configurational partition function of a mixture of biaxial HRP on a simple cubic lattice by applying the orientation dependent version of Flory–Huggins statistics. The limit of infinitesimal mesh size has been considered as the corresponding off-lattice model. We discuss the accuracy of the EOS and for the case of a binary mixture of uniaxial platelets we view the interrelations between the EOS of the present approach and that of the FMT [19]. In the third section, the model is employed in the study of phase behaviour and orientational properties of bidisperse hard-rod fluids and bidisperse hard-platelet fluids, forming isotropic and nematic phases. Apart from getting novel information about special features of the phase diagram of hard-particle mixtures, this study was aimed at comparison with results of continuous orientation approach [7]. Section 4 presents conclusions.

2. Lattice and off-lattice versions of the Zwanzig model (y^3 level)

2.1. *Equation of state*

We consider a $k-$component mixture of rectangular parallelepipeds on a simple cubic lattice. The lattice has M cells and each cell has a volume $\Delta v = x^3$, where x is the length of an edge. Component k consists of particles with volume v_k and with dimensions $A_{1k} \times A_{2k} \times A_{3k}$. In general each particle may take up six orientations, corresponding to the alignment of the particle's principal axes with those of the lattice (figure 1). The notation for the labeling of these orientations is shown in figure 1. For a given component, k, we denote the fraction of those particles which have an orientation α by $s_{\alpha k}$. Thus, if N_k is the number of particles of type k and $N_{\alpha k}$ is the number of particles of type k with orientation α, then $s_{\alpha k} = N_{\alpha k}/N_k$ and clearly $\sum_{\alpha=1}^{6} s_{\alpha k} = 1$. A particle of type k occupies $r_k = \prod_{i=1}^{3} r_{\alpha k}^{(i)}$ adjacent lattice cells. Here, $r_{\alpha k}^{(i)}$ is the number of cells that make up the ith edge of a particle of type k and orientation α. The ith edge is that edge which is aligned along lattice axis i.

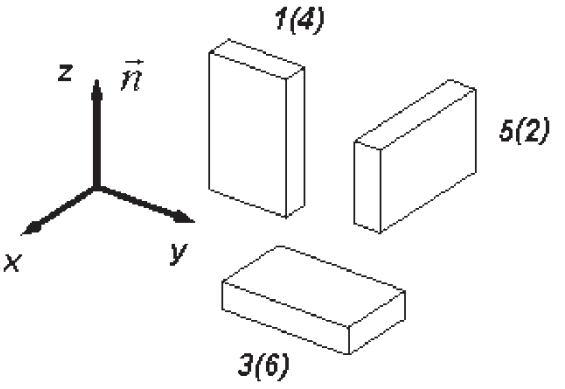

Figure 1. Allowed orientations of a cuboidal particle on a cubic lattice. In the nematic phase we take the director $\vec{n}$ to be parallel to the z-axis. Orientations labelled by indices in parentheses may constructed by rotation of those, which are drawn, about molecule axes A_1, A_2 and A_3 through $\pi/2$.

The configurational contribution to the Helmholtz energy takes the form [26]

$$\beta F_{latt} = -\ln\left[\frac{(\Delta v)^N \cdot g_d\,(\{N_\lambda\};\, M)}{6^N \prod_k \prod_{\alpha=1}^{6} N_\lambda!}\right], \qquad (1)$$

where $g_d(\{N_\lambda\};M)$ is the total number of ways to arrange $\{N_\lambda\}$ distinguishable particles on M lattice sites, $\beta = 1/k_B T$ and the index $\lambda \equiv \alpha k$ labels a particle of type k and orientation α ($1 \le \lambda \le 6k$). In the thermodynamic limit, $g_d(\{N_\lambda\};M)$ is minimized with respect to variables $\{s_{\alpha k}\}$.

Approximate methods to estimate g_d have been given previously [22, 23, 26–28]. Except for linear rods, however, these methods suffer from the problem that the value obtained for g_d depends upon the order in which the particles are placed on the lattice, which is unphysical and thermodynamically inconsistent. An improved methodology has been developed for hard rectangles on a square lattice [29] and this has been shown to give thermodynamically consistent results. We now generalize this result for parallelepipeds.

We first review the earlier Flory–DiMarzio–Alben counting schemes. If $\{X_\lambda\}$ particles have already been placed on the lattice, one has to estimate the number of configurations, $\nu_\lambda(\{X_\lambda\};X_\lambda+1)$, available for the $(X_\lambda+1)$ th particle of type λ. This can be done using the following approximation:

$$\nu_\lambda(\{X_\lambda\};\, X_\lambda+1) = X_0 \bar{P}(\{X_\lambda\};(r_\lambda - 1)) = X_0 \bar{P}_\lambda, \qquad (2)$$

where $X_0 (= M - \sum_\lambda X_\lambda r_\lambda, \quad r_\lambda \equiv r_k)$ is the number of vacant cells which can accommodate one of the corner segments of the new block to be placed on the lattice.

$\bar{P}_\lambda$ is the probability of finding all $r_\lambda - 1$ adjacent lattice cells vacant, so there is space to insert the whole particle, given the positioning of the corner.

As in our earlier studies [29, 30], we shall seek expressions for v_λ, which satisfy the reciprocity relations:

$$\left(\frac{\partial \ln v_\lambda}{\partial X_\delta}\right)_{T,M,\{X_{\lambda\neq\delta}\}} = \left(\frac{\partial \ln v_\delta}{\partial X_\lambda}\right)_{T,M,\{X_{\delta\neq\lambda}\}}, \tag{3}$$

where v_λ is related to g_d, in the thermodynamic limit, by

$$\ln v_\lambda = \frac{\partial \ln g_d(\{X_\lambda\}; M)}{\partial X_\lambda}. \tag{4}$$

Equation (3) can be re-written in terms of a Maxwell relationship between chemical potentials, $\mu_\lambda^{\text{latt}} = \partial F_{\text{latt}}/\partial X_\lambda$, i.e.

$$\left(\frac{\partial \mu_\lambda^{latt}}{\partial X_\delta}\right)_{T,V,\{X_{\lambda\neq\delta}\}} = \left(\frac{\partial \mu_\delta^{latt}}{\partial X_\lambda}\right)_{T,V,\{X_{\delta\neq\lambda}\}}, \tag{5}$$

where $V = M\Delta v$ is the volume of the system.

Relations (3) and (5) provide a criterion for the thermodynamic consistency of one's expression for $g_d(\{N_\lambda\};M)$ and the free energy F_{latt} [26].

In order to compute the probability $\bar{P}_\lambda$, defined in equation (2), we follow Flory and introduce the quantity P_n. This is the conditional probability that an empty cell has an empty neighbour along a direction $\vec{n}$. Assuming a random distribution of empty and occupied cells, one obtains

$$P_n = \frac{X_0}{X_0 + B_n}, \tag{6}$$

where B_n is the number of particle segments which could possibly occupy a cell in that direction.

For the case of parallelepipeds, possible directions of $\vec{n}$ are shown in figure 2. If the unit vectors $\vec{i}, \vec{j}$ and $\vec{k}$ are co-linear with the lattice axes, then the vector $\vec{n}$ may be

1. parallel to $\vec{i}$, $\vec{j}$ or $\vec{k}$ (contacts of type 'a', $n = 1, 2,$ or 3);
2. parallel to $\vec{i} \pm \vec{j}$, $\vec{i} \pm \vec{k}$ or $\vec{j} \pm \vec{k}$ (contacts of type 'b', $n = 12, 13,$ or 23);
3. parallel to $\vec{i} \pm \vec{j} \pm \vec{k}$ (contacts of type 'c', $n = 123$).

The symmetry of the system dictates that the directions $\vec{n}$ and $-\vec{n}$ are equivalent, so $B_{\vec{n}} = B_{-\vec{n}}$. In the case of type 'b' contacts, we have $B_{\vec{i}+\vec{j}} = B_{\vec{i}-\vec{j}}$, $B_{\vec{i}+\vec{k}} = B_{\vec{i}-\vec{k}}$, $B_{\vec{j}+\vec{k}} = B_{\vec{j}-\vec{k}}$, while for case 'c' all possible $B_{\vec{n}}$ are equal. In later discussion, when each types of contact is treated explicitly, we replace the subscripts in $B_{\vec{n}}$ and $P_{\vec{n}}$ by the numerical indices shown in figure 2.

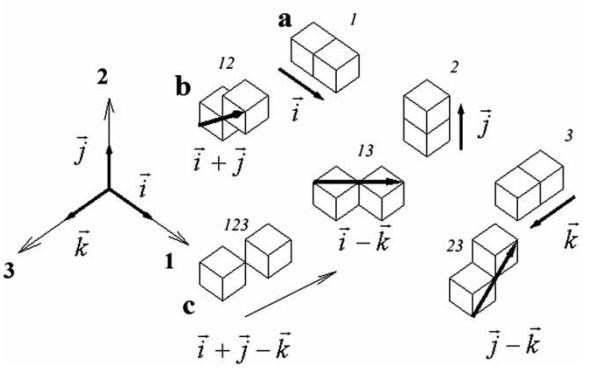

Figure 2. Layout of the cell adjacencies on a lattice, indicating connections via a common facet (a), an edge (b) or a vertex (c). As shown on the figure, each site adjacency is characterized by a combination of the lattice primitive vectors $\{\vec{i},\vec{j},\vec{k}\}$. The number beside the pair of sites in contact indicates a direction with respect to the lattice frame and is used in the text to define probability of the vacancy/occupancy state of a cell.

Expressions for B_n may be obtained by simple geometric reasoning. First, consider case 'a' where we view along a direction $i (i = 1, 2$ or 3) from an empty lattice cell taken at random. The only way that the neighboring cell could be occupied by a particle with orientation λ is if the cell were occupied by a segment belonging to the face normal to the direction i. The number of segments in such a face is $r_\lambda^{(j)} \cdot r_\lambda^{(k)} = r_\lambda / r_\lambda^{(i)}$. If one multiplies this quantity by the number of particles X_λ and then sums over all values of λ, one obtains an expression for B_i in the form

$$B_i = \sum_\lambda \frac{X_\lambda r_\lambda}{r_\lambda^{(i)}}. \tag{7.1}$$

We now turn to case 'b', in which we move from an empty cell in directions 12, 13 or 23. If the neighboring cell is occupied by a particle of orientation λ, then this may be due to any segment on two faces of the particle. For the general direction ij, the total number of such segments is $r_\lambda^{(i)} r_\lambda^{(k)} + r_\lambda^{(j)} r_\lambda^{(k)} - r_\lambda^{(k)}$. The last term is subtracted to avoid the double counting of the segments on the common edge that is parallel to k. In this case the expression for B_{ij} is

$$B_{ij} = \sum_\lambda X_\lambda r_\lambda \left(\frac{1}{r_\lambda^{(i)}} + \frac{1}{r_\lambda^{(j)}} - \frac{1}{r_\lambda^{(i)} r_\lambda^{(j)}}\right). \tag{7.2}$$

Finally, we come to case (3) and consider a move from an empty cell in the direction 123. If this cell is

occupied by a particle with orientation λ, this may be due to cells on all three faces of the particle. The number of such cells is $r_\lambda - \prod_{i=1}^{3}(r_\lambda^{(i)} - 1)$. Thus, for B_{123} we have:

$$B_{123} = \sum_\lambda X_\lambda \left[r_\lambda - \prod_{i=1}^{3} \left(r_\lambda^{(i)} - 1 \right) \right]. \tag{7.3}$$

As was shown earlier, the Flory–DiMarzio–Alben statistics violates the condition of thermodynamic consistency when applied to a system of 2D and 3D hard particles [29, 30]. To avoid this problem, the counting scheme has to take more care about taking into account the occupancy/vacancy states of adjacent lattice cells needed to accommodate the segments of facets and the interior of the $(X_\lambda + 1)$ th particle. To do this, we introduce the conditional probability, $P^*_{i,j,k}$, that a given lattice cell is vacant given that the adjacent cells in the directions i, j and k are simultaneously vacant. As is shown in figure 2, each of these indices can take the values 1, 2, 3, 12, 23, 13. We assume, that if $j = k$ or $i = k$ one has: $P^*_{i,j,k} = P^*_{i,j,j} = P^*_{i,j}$ and $P^*_{i,j,i} = P^*_{i,j}$ if $i = j = k$ it holds: $P^*_{i,i,i} = P_i$. In the case of rigid one-dimensional objects when one considers only contacts of type 'a', i takes the values 1, 2 or 3.

To proceed, we express the probabilities $P^*_{i,j,k}$ in terms of P_n, defined in equation (6). Let first consider the case $i = 1$ and $j = 2$. We define the probability $P^*_{1,2}$ as follows:

$$P^*_{1,2} = \frac{X_0 P_1 P_2}{X_0 P_{12}} = \frac{P_1 P_2}{P_{12}}, \tag{8}$$

where $X_0 P_{12}$ is the average number of cells in pairs with adjacency implemented as is shown in figure 3 (a′), the cross-marked cell (figure 3 (b′)) being either vacant or occupied. The product $X_0 P_{12}$ corresponds to the average number of cells, which can be either vacant or occupied, whose neighbours in the directions 1 and 2 are vacant. Similarly, the product $X_0 P_1 P_2$ is the average number of three vacant adjacent cells as is shown in figure 3 (b′). Then, the ratio of $X_0 P_1 P_2$ and $X_0 P_{12}$ can be equated to the probability of finding a given cell empty provided two adjacent cells in the directions 1 and 2 are also empty.

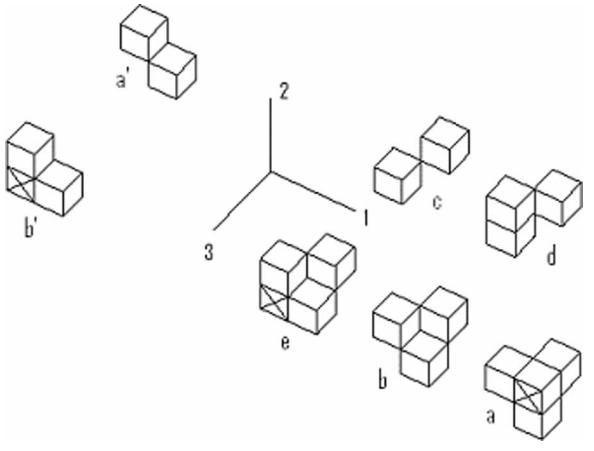

Figure 3. Adjacencies of the lattice sites explaining the definition of the conditional probabilities $P^*_{1,2}$ and $P^*_{1,2,3}$.

In general one has:

$$P^*_{i,j} = \frac{X_0 P_i P_j}{X_0 P_{ij}} = \frac{P_i P_j}{P_{ij}}. \tag{9}$$

The indices on the r.h.s. can only be 1, 2 or 3. For $P^*_{i,j}$ the indices span the set $i, j = 1; 2; 3; 12; 13; 23$. The indices may not both be two figure indices (e.g. $P^*_{12,13}$ is not permitted).

Analogous to the definition of $P^*_{i,j}$ discussed above, we consider now the probability $P^*_{1,2,3}$ of finding a vacant 4-particle cluster of configuration a (figure 3). Let the quantity A_1 be the number of vacant cells, whose neighbours in the directions 1, 2 and 3 are also vacant. Making use of Flory's definition of P_n (equation (6)), one gets: $A_1 = X_0 P_1 P_2 P_3$. It then follows that $P^*_{1,2,3} = A_1 / A_2$, where the quantity, A_2, is the average number of 3-cell clusters of vacancies (case b in figure 3), which are adjacent to a cross-marked cell shown in configuration a, whether this cell is empty or occupied.

To proceed, the probability of finding a cluster with configuration b ought to be connected with the previously defined probabilities P_{ij} and P_{123}. We consider clusters of vacancies with configurations c, d, e (figure 3). We denote their average numbers by A_3, A_4 and A_5, respectively. It then follows that

$$\begin{aligned} A_3 &= X_0 P_{123} \\ A_4 &= A_3 P^*_{2,13} = X_0 P_{123} P^*_{2,13} \\ A_5 &= A_4 P^*_{1,23} = X_0 P_{123} P^*_{2,13} P^*_{1,23}. \end{aligned}$$

Alternatively, A_5 is related to A_2 by $A_5 = A_2 P^*_{1,2}$, where $P^*_{1,2}$ is the probability that two neighbouring cells of a cross-marked one (configuration e), in the directions 1 and 3, are empty.

Substituting $A_2 = A_5 / P^*_{1,2}$ and $A_5 = X_0 P_{123} P^*_{2,13} P^*_{1,23}$ into the definition of $P^*_{1,2,3}$ and making use of equation (9) we get:

$$P^*_{1,2,3} = \frac{P_1 P_2 P_3 P_{123}}{P_{12} P_{13} P_{23}}. \tag{10}$$

By using (9) and (10), ν_λ can be written in the following form:

$$\nu_\lambda = X_0 \prod_{i=1}^{3} P_i^{\left(r_\lambda^{(i)}-1\right)} \prod_{i<j}^{3} \left(P_{i,j}^*\right)^{\left(r_\lambda^{(i)}-1\right)\left(r_\lambda^{(j)}-1\right)} \times \left(P_{1,2,3}^*\right)^{\prod_{i=1}^{3}\left(r_\lambda^{(i)}-1\right)}. \quad (11)$$

Here, the product $X_0 P_1^{\left(r_\lambda^{(1)}-1\right)}$ can be interpreted as the average number of vacant cells having $(r_\lambda^{(1)}-1)$ contiguous neighboring lattice cells in the direction 1 vacant; $X_0 P_1^{\left(r_\lambda^{(1)}-1\right)} P_2^{\left(r_\lambda^{(2)}-1\right)}$ is the average number of vacant lattice cells whose contiguous $(r_\lambda^{(1)}-1)$ and $(r_\lambda^{(2)}-1)$ adjacent cells in the directions 1 and 2, respectively, are empty, etc.

Now we show that the quantities ν_λ obey the self-consistency criterion, equation (3). In view of relationships (8)–(10), expression (11) can be rearranged to give:

$$\nu_\lambda = \frac{X_0^{r_\lambda} \prod_{i<j}^{3} \left[X_0 + B_{ij}\right]^{r_\lambda\left(1-1/r_\lambda^{(i)}\right)\left(1-1/r_\lambda^{(j)}\right)}}{\left[X_0 + B_{123}\right]^{\prod_{i=1}^{3}\left(r_\lambda^{(i)}-1\right)} \prod_{i=1}^{3} \left[X_0 + B_i\right]^{r_\nu\left(1-1/r_\lambda^{(i)}\right)}}. \quad (12)$$

After straightforward manipulations one finds:

$$\frac{\partial \ln \nu_\lambda}{\partial X_\delta} = \frac{\prod_{i=1}^{3}\left(r_\lambda^{(i)}-1\right)\left(r_\delta^{(j)}-1\right)}{X_0 + B_{123}} + \sum_{i=1}^{3} \frac{r_\lambda r_\delta \cdot \left(r_\lambda^{(i)}-1\right)\left(r_\delta^{(i)}-1\right)}{r_\lambda^{(i)} r_\delta^{(i)} \cdot \left(X_0 + B_i\right)} - \sum_{\substack{i<j \\ l\neq i,j}}^{3} \frac{r_\lambda^{(l)} r_\delta^{(l)} \cdot \prod_{i=1}^{3}\left(r_\lambda^{(i)}-1\right)\left(r_\delta^{(i)}-1\right)}{\left(r_\lambda^{(l)}-1\right)\left(r_\delta^{(l)}-1\right)\left(X_0 + B_{ij}\right)} - \frac{r_\lambda r_\delta}{X_0}. \quad (13)$$

It is obvious that relation (13) is symmetric with respect to permutation of the subscripts λ and δ. Thus, the Maxwell relation (equation (3)) is satisfied, providing a condition of integrability of the following equation for the calculation of the combinatorial factor g_d:

$$\ln g_d(\{N_\lambda\}) = \int_0^{N_1} \ln \nu_1(X_1) dX_1 + \int_0^{N_2} \ln \nu_2(N_1; X_2) dX_2 + \cdots + \int_0^{N_\lambda} \ln \nu_\lambda(\{N_\beta\}_{\beta<\lambda}; X_\lambda) dX_\lambda. \quad (14)$$

Using equation (12), integrating equation (14) making use of Stirling's approximation and finally replacing X_λ in equation (7) with $N_{\alpha k}$ yields:

$$g(\{N_\lambda\}) = \frac{\left(N_0 + B_{123}\right)! \prod_{i=1}^{3}\left(N_0 + B_i\right)!}{N_0! \prod_\lambda N_\lambda! \prod_{i<j}^{3}\left(N_0 + B_{ij}\right)!}, \quad (15)$$

where $N_0 = M - \sum_k N_k r_k$ and the expressions for B_i, B_{ij} and B_{123} are obtained from equation (7) by replacing X_λ with N_λ.

According to (1) and (15), the equation of state of the multi-component fluid under consideration takes the form:

$$\beta P \Delta v = \frac{\left(N_0 + B_{123}\right) \prod_{i=1}^{3}\left(N_0 + B_i\right)}{N_0 \prod_{i<j}^{3}\left(N_0 + B_{ij}\right)}. \quad (16)$$

The generalization to continuous translational space is achieved by following the procedure previously devised for the hard rectangle fluids [29]. For a 3D lattice system of parallelepipeds, we gave details of derivation earlier [31; (1997)]. It can be performed by taking the limit ($z = x/a$ is the dimensionless edge of a cubic lattice cell, a is the unit length):

$$F_{\text{conf}} = \lim_{z\to 0} F_{\text{latt}}. \quad (17)$$

Combining equations (1), (15) and performing the necessary transformations in (17) one obtains the following expression for the configurational Helmholtz energy, $F_{\text{conf}}(\{N_{\alpha k}\})$, of an athermal multi-component fluid of particles with D_{2h} symmetry:

$$\beta F_{\text{conf}}(\{N_{\alpha k}\}) = \sum_k N_k \left\{ \sum_\alpha s_{\alpha k}(\ln s_{\alpha k} - 1) + \ln \frac{\varphi_k / v_k}{\bar{V} - 1} + f_k \left[\frac{1}{(\bar{V}-1)} \sum_{i=1}^{3} a_i b_i + \frac{1}{(\bar{V}-1)^2} \prod_{i=1}^{3} a_i \right] \right\} \quad (18)$$

Here, $\varphi_k = N_k v_k / \sum_l N_l v_l$ is the volume fraction of component k, $\eta = \sum_l N_l v_l / V$ is the packing fraction, $\overline{V} = 1/\eta$, $a_i \equiv \sum_k \varphi_k \sum_\alpha s_{\alpha k} / f_{\alpha k}^{(i)}$, $b_i \equiv \sum_k \varphi_k \sum_\alpha s_{\alpha k} f_{\alpha k}^{(i)} / f_k$, $f_k = v_k / a^3$ and the quantity $f_{\alpha k}^{(i)} = r_{\alpha k}^{(i)} z$ is the dimensionless length of an edge of a particle of type k with orientation α constrained along the direction i.

To determine the equilibrium orientational distribution of particles, one has to minimize F_{conf} with respect to $\{N_{\alpha k}\}$ or to $\{s_{\alpha k}\}$ while maintaining the constraint $\sum_{\varepsilon=1}^{6} N_{\alpha k} = N_k$ or, equivalently, $\sum_{\varepsilon=1}^{6} s_{\alpha k} = 1$. If a nematic phase composed of biaxial particles has biaxial symmetry, it implies that the number of variables necessary for minimizing the functional (18) is equal to $5k$, and $s_{1k} \neq s_{2k} \neq \cdots \neq s_{6k}$. In this case, if one chooses s_{6k} as independent variables, equilibrium values $\{s_{\alpha k}\}$ may be located from the following set of equations:

$$\beta \left(\frac{\partial F_{\text{conf}}}{\partial N_{\alpha k}} \right)_{\{N_k\}} = \mu_{\alpha k} - \mu_{6k} = 0, \quad (19)$$

where

$$\beta\mu_{\alpha k} = \beta\left(\frac{\partial F_{conf}}{\partial N_{\alpha k}}\right)_{V,\{N_{\beta\neq\alpha}\}} = -1 + \beta P v_k + \ln\frac{\varphi_k\eta}{v_k(1-\eta)} + \ln s_{\alpha k} + \frac{f_k\eta}{1-\eta}\sum_{i=1}^{3}\left[a_i\frac{f_{\alpha k}^{(i)}}{f_k} + b_i\frac{1}{f_{\alpha k}^{(i)}}\right] + \frac{f_k\eta^2}{(1-\eta)^2}\prod_{i=1}^{3}a_i\sum_{i=1}^{3}\frac{1}{a_i f_{\alpha k}^{(i)}} \quad (20)$$

is a chemical potential of a particle of kind k with orientation α, and

$$\beta P a^3 = -\beta a^3\left(\frac{\partial F_{conf}}{\partial V}\right)_{T,\{N_{\alpha k}\}} = \frac{\rho a^3}{1-\eta} + \frac{\eta^2}{(1-\eta)^2}\sum_{i=1}^{3}a_i b_i + \frac{2\eta^3}{(1-\eta)^3}\prod_{i=1}^{3}a_i \quad (21)$$

is the dimensionless pressure, $\rho = \sum_k N_k/V$ is the number density.

At equilibrium, the following identities are also necessarily obeyed:

$$\mu_k = \mu_{\alpha k},\ \alpha = 1,\ldots,6, \quad (22)$$

where $\mu_k = (\partial F_{conf}/\partial N_k)_{T,V,N_{l\neq k}}$ is the chemical potential per molecule of component k.

In uniaxial nematics with D_{2h} particles, symmetry considerations (see figure 1) imply that $s_{1k} = s_{4k}$, $s_{2k} = s_{5k}$, $s_{3k} = s_{6k}$, which means that the set (19) contains $2k$ equations. For square cross-section parallelepipeds there are k equations in the set (19).

Expressions (18)–(21) are thermodynamically consistent in that equations (3), (4) and (5) have been obeyed. This model permits the study of multi-component mixtures of biaxial particles, with the possibility of predicting a biaxial nematic phase. Although the model does not allow for continuous orientations, it does have the advantage that one is dealing with sets of non-linear algebraic equations rather than a system of nonlinear integral equations. As was pointed out in the introduction, the Zwanzig approximation provides qualitatively accurate accounts of a variety of properties of nematic mixtures as well as of non-uniform systems [33, 34]. In order, however, to give an accurate account of soft phase transitions, as is the case for real liquid crystal systems, orientations need to be treated as continuous variables. Order parameters of higher order than the second play a dominant role in determining the nature and features of the nematic-isotropic transition [35]. These effects are not present in the restricted orientation model studied here.

2.2. *Comparison of the EOS of the uniform system with those obtained from other approaches*

As mentioned in the Introduction, the EOS derived in the previous section is identical to that derived previously using seemingly completely different sets of approximations. First, we note the work of Mitra and Allnatt [36] who obtained this EOS by retaining only the full Mayer star diagrams in the virial expansion and then summing the series. Some details of their approach are given in Appendix 1.

Second, we consider the results obtained by applying FMT to systems of hard rectangular particles [18–20]. For the sake of future comparison we focus on the case of a binary fluid of square platelets with dimensions $L_k \times D_k \times D_k$ ($L_k < D_k$, $k = 1, 2$). The FMT EOS of such a fluid has been derived in [19] by generalizing Cuesta's result for hard parallel cubes [17] and used to study isotropic-nematic interfaces and the phase behaviour of model lamellar colloids.

The FMT expression for the reduced free energy density of a mixture is given by $\Phi_{conf} = \Phi_{id} + \Phi_{ex}$, where the ideal part, Φ_{id}, has the form

$$\Phi_{id} = \sum_{k,\alpha}\rho_\alpha^{(k)}(\ln\rho_\alpha^{(k)} - 1), \alpha = x,y,z, \quad (23)$$

while the excess free energy density is represented by the following equation:

$$\Phi_{ex} = -n_0\ln(1-n_3) + \frac{\vec{n}_1\cdot\vec{n}_2}{1-n_3} + \frac{n_{2,x}n_{2,y}n_{2,z}}{(1-n_3)^2}. \quad (24)$$

In (23) and (24), according to [19], in the case of a homogeneous bulk fluid the density variables $\{n_i\}$ are determined as

$$n_0 = \sum_{k=1}^{2}(\rho_x^{(k)} + \rho_y^{(k)} + \rho_z^{(k)}),$$

$$\vec{n}_1 = \sum_{k=1}^{2}\begin{pmatrix} L_k\rho_x^{(k)} + D_k\rho_y^{(k)} + D_k\rho_z^{(k)} \\ D_k\rho_x^{(k)} + L_k\rho_y^{(k)} + D_k\rho_z^{(k)} \\ D_k\rho_x^{(k)} + D_k\rho_y^{(k)} + L_k\rho_z^{(k)} \end{pmatrix}$$

$$\vec{n}_2 = \sum_{k=1}^{2}\begin{pmatrix} D_k\rho_x^{(k)} + L_k\rho_y^{(k)} + L_k\rho_z^{(k)} \\ L_k\rho_x^{(k)} + D_k\rho_y^{(k)} + L_k\rho_z^{(k)} \\ L_k\rho_x^{(k)} + L_k\rho_y^{(k)} + D_k\rho_z^{(k)} \end{pmatrix} D_k$$

$$n_3 = \sum_{k=1}^{2}L_k D_k^2(\rho_x^{(k)} + \rho_y^{(k)} + \rho_z^{(k)}),$$

Here, $\rho_\alpha^{(k)}$ is the number density of platelets of species k with orientation α and $n_{2,\alpha}$ is the projection of the vector $\vec{n}_2$ in the α $(=x,y,z)$ direction. Insofar as within the Zwanzig model the orientational distribution function for the species k is defined by the set of fractions $s_{\alpha k}$, the number densities are $\rho_\alpha^{(k)} = N_k s_{\alpha k}/V$, $\sum_\alpha \rho_\alpha^{(k)} = \rho_k$.

Now consider the free energy density of the fluid in terms of the present approach. According to equation (18) it may be brought to the form:

$$\frac{\beta F_{conf}(\{N_{\alpha k}\})}{V} = \sum_k \rho_k \left[-1 + \ln \rho_k + \sum_{\alpha=1}^{n} s_{\alpha k} \ln s_{\alpha k} \right] + \left(\frac{\beta F_{ex}(\{N_{\alpha k}\})}{V} \right), \tag{25}$$

where the first term, $\beta F_{id}/V = \Phi_{id}$, is the ideal part (with $\rho_\alpha^{(k)} = N_k s_{\alpha k}/V$, $\sum_\alpha \rho_\alpha^{(k)} = \rho_k$, $n_0 = \sum_k \rho_k$), and $F_{ex}(\{N_{\alpha k}\})/V$ is the excess free energy density of a fluid with restricted orientations of particles, relative to an ideal multi-component hard-platelet mixture:

$$\frac{\beta F_{ex}(\{N_{\alpha k}\})}{V} = \sum_k \rho_k \left[-\ln(1-\eta) + f_k \left(\frac{\eta}{1-\eta} \sum_{i=1}^{3} a_i b_i + \frac{\eta^2}{(1-\eta)^2} \prod_{i=1}^{3} a_i \right) \right]. \tag{26}$$

Expressing a_i and b_i in the form

$$a_i = \left(\sum_{k=1}^{2} N_k f_k \right)^{-1} \sum_{k=1}^{2} N_k \sum_{\alpha=1}^{3} \frac{s_{\alpha k} f_k}{f_{\alpha k}^{(i)}},$$

$$b_i = \left(\sum_{k=1}^{2} N_k f_k \right)^{-1} \sum_{k=1}^{2} N_k \sum_{\alpha=1}^{3} s_{\alpha k} f_{\alpha k}^{(i)},$$

equation (26) can be written in the form (with $\tilde{f}_{\alpha k}^{(i)} = f_{\alpha k}^{(i)} a$):

$$\frac{\beta F_{ex}\{N_{\alpha k}\}}{V} = \rho \ln \frac{1}{1-\eta} + \frac{\sum_{i=1}^{3} \left(\sum_{k,\alpha} \rho_\alpha^{(k)} \tilde{f}_{\alpha k}^{(i)} \right) \left(\sum_{k,\alpha} \rho_\alpha^{(k)} v_k / \tilde{f}_{\alpha k}^{(i)} \right)}{1-\eta} + \frac{\prod_{i=1}^{3} \sum_{k,\alpha} \rho_\alpha^{(k)} v_k / \tilde{f}_{\alpha k}^{(i)}}{(1-\eta)^2}. \tag{27}$$

In accordance with the chosen labelling of orientations (elements $i = 1, 2, 3$ correspond, respectively, to the directions along the axis x, y and z, the plate director lies along the z axis), the geometric characteristics of the particles, $v_k/\tilde{f}_{\alpha k}^{(i)}$ and $\tilde{f}_{\alpha k}^{(i)}$, are given by the following elements:

i \ α	$v_k/\tilde{f}_{\alpha k}^{(i)}$			$\tilde{f}_{\alpha k}^{(i)}$		
	1	5	3	1	5	3
1	$D_k D_k$	$L_k D_k$	$L_k D_k$	L_k	D_k	D_k
2	$L_k D_k$	$D_k D_k$	$L_k D_k$	D_k	L_k	D_k
3	$L_k D_k$	$L_k D_k$	$D_k D_k$	D_k	D_k	L_k

Making use of the data in the table, it is straightforward to show the equivalence of equations (24) and (27). The identity of the free energy expressions means that for spatially homogeneous bulk phases both our approach and FMT predict identical phase diagrams and thermodynamic properties.

Third, the EOS is identical to that given by the y^3-expansion [21], which requires as input the values of all partial second and third virial coefficients. Although the calculation of these quantities is possible for restricted orientation models, as the Mayer functions reduce to products of Heaviside step functions, the direct computation of these coefficients in multi-component mixtures of biaxial particles turns out to be cumbersome. In contrast, the present approach avoids the need to directly evaluate the virial coefficients.

Finally, we review the differences between lattice and off-lattice versions of the model, by comparing the values of the virial coefficients B_n in a one-component fluid of parallel hard cubes. These have been calculated up to the seventh order [37]. The data given in Appendix 2 show that discretizing the positions of the particles strongly affects the B_n values and considerably weakens the role of steric repulsions. In the context of this observation it is important to remember that the discretization of particle positions in lattice approximations may lead to incorrect inferences about the relative stabilities of smectic and columnar phases when studying translational ordered liquid-crystalline systems [38].

3. Applications

In this section, we focus on the analysis of novel characteristics relating to the stability of nematic and isotropic phases in mixtures of rods and in mixtures of plates. We make comparisons with previous theoretical studies of freely rotating hard cylinders [7].

3.1. *Isotropic–nematic transition and fluid–fluid de-mixing in related rod–rod and plate–plate mixtures (composed of particles with equal aspect ratios)*

Here, we present results obtained by applying the model to binary rod–rod and binary plate–plate mixtures. In each case, the two components differ substantially in volume and aspect ratio. The volume and the aspect ratio of the thicker rods (R_1) are chosen to be identical to those of the thicker plates (P_1), and the same holds for the thin rods (R_2) and thin plates (P_2). Thus, at the second virial level of description, the pure R_1 and P_1 systems are identical, as are the pure R_2 and P_2 systems. For long thin rods the third virial contribution is negligible. This is not, however, the case for plates, no matter how thin [5, 9]. We may illustrate this for the case of one-component isotropic fluids composed of cuboids with dimensions $L \times D \times D$ We compare the ratio B_3/B_2^2 (B_n is the nth-order virial coefficients) for rods and plates with various aspect ratios $\Gamma = L/D$.

Γ	10	1/10	15	1/15	150	1/150	∞	0
B_3/B_2^2	0.2791	0.3463	0.2119	0.3013	0.0279	0.1839	0	1/6

The isotropic values of B_2 and B_3 are given by [19, 21, 31; (1997)]:

$$\frac{B_2}{v} = \frac{1}{3}(\Gamma + 2)(\Gamma^{-1} + 2) + 1, \tag{28}$$

$$\frac{B_3}{v^2} = \frac{1}{9}\left(\frac{2}{3\Gamma^2} + \frac{16}{\Gamma} + \frac{52\Gamma}{3} + 47\right). \tag{29}$$

It is evident that at intermediate aspect ratios the virial expansion converges slowly, and, especially for platelets, the triplet interactions can never be ignored. For continuous orientation models, the ratio B_3/B_2^2 was estimated to be 0.51 for hard discs with an aspect ratio of 0.1 [39; (1992)] and 0.313 for spherocylinders with an aspect ratio of 10 [39; (1987)]. In these models higher virial terms can be approximately incorporated into Onsager's theory by rescaling the second virial term; this method has been generalized to cater for mixtures of particles with low and intermediate aspect ratios [7–9].

In view of these results it is obvious that one needs to exploit more rapidly convergent expansions. As was shown in the previous section, our model gives the third $y-$ expansion expression with exact third virial coefficients for mixtures of hard cuboids. In the context of recent statistical thermodynamic and experimental studies of hard-rod [1, 7–11] and platelet [9, 19, 20] mixtures, it gives grounds for a comparative study of the behaviour of mixtures, the different phase behaviour being caused by the difference of shape of particles with the same volume. This circumstance could be studied on the basis of a single statistical thermodynamic approach. To this end we considered the said two series of binary hard-particle mixtures. The first is the $R_1 - R_2$ mixture, consisting of rods with dimensions $L_{iR} \times D_{iR} \times D_{iR}$ ($\Gamma_{iR} = L_{iR}/D_{iR}, \Gamma_{iR} > 1$), whilst the second one is a $P_1 - P_2$ mixture, composed of platelets $L_{iP} \times D_{iP} \times D_{iP}$ ($\Gamma_{iP} = L_{iP}/D_{iP}, \Gamma_{iP} < 1$). It is of particular interest to compare systems for which $v_{iR} = v_{iP}$ and $\Gamma_{iR} = \Gamma_{iP}^{-1}$, as any differences must be due to higher order effects than the second virial coefficients.

We study systems in which $\Gamma_{1R} = 15$ and $\Gamma_{1P} = 1/15$. To ensure equal volumes, we must have $D_{1P} = 15^{2/3} D_{1R} = 6.0822 D_{1R}$. For the second, thin components we set the aspect ratios to be 150 and 1/150 accordingly. D_{2R} was fixed at unity, so for equal volumes we must have $D_{2P} = 150^{2/3} = 28.231$. D_{1R} was varied between 2 and 50. Consequently, given equal volumes for P_1 and R_1, the ratio of the widths of the two plates was given by $D_{1P}/D_{2P} = 0.1^{2/3} D_{1R}/D_{2R} = 0.21544 D_{1R}$. Given these choices for the geometrical parameters of the species, only the ratio $d_R = D_{1R}/D_{2R}$ may be varied.

It should be noticed that the average aspect ratios of real prototypes of hard particles, such as a rodlike boehmite colloid and a platelike gibbsite colloid, have values of about 10–20 and 1/15 [1, 11 (2000)]. Although a rod aspect ratio of 150 does not seem realistic in this context, rod mixtures with these particular sets of molecular parameters are chosen because of an opportunity to compare our results with the recent study of hard freely rotating cylinders with aspect ratios of 15 and 150 [7]. The underlying theory was a Parsons–Lee extension of Onsager theory. A binary blend of hard spherocylinders with the same aspect ratio had previously been studied by Gibbs ensemble Monte Carlo simulations [40]. Our focus is first to compare features of the $N - I$ phase coexistence in $R_1 - R_2$ and $P_1 - P_2$ mixtures for small concentrations of component 2 – i.e. component 2 is dissolved in excess liquid crystal solvent (mimicked by component 1). We also aimed to study fluid–fluid phase separation as a function of the particle volume ratio. In addition to this, for a number of $R_1 - R_2$ blends we investigate the stability of an $I - I$ demixing with respect to the $N - I$ transition.

3.2. *Calculation procedure*

Calculation of the limiting slopes of coexisting nematic (N) and isotropic (I) phases, $\beta_{2,\infty}^{(r)} = -\lim_{x_2 \to 0} d(t^*)^{(r)}/dx_2$, ($r = I,N$), in the vicinity of component 1 was performed in terms of the reduced temperature (identical

to the dimensionless inverse pressure) defined as $t^* = (P_1^*)_{NI}/(Pv_1/k_BT)$, where $(P_1^*)_{NI} = (Pv_1/k_BT_1)_{NI}$ is the reduced coexistence pressure of component 1. The limiting slopes can be determined by applying the thermodynamic relationship [40]:

$$\beta_{2,\infty}^{(q)} = \left(\frac{k_B}{\Delta\Sigma_1^{(NI)}}\right)\left[\frac{\gamma_{2,\infty}^N - \gamma_{2,\infty}^I}{\gamma_{2,\infty}^{(r)}}\right] \quad (q \neq r;\ q,r = I,N), \tag{30}$$

where

$$\gamma_{2,\infty}^{(r)} = \exp\left[\lim_{x_2\to 0}(\beta\mu_2^{(r)} - \ln x_2) - \beta\mu_2^0\right] \tag{31}$$

is the limiting activity coefficient of a solute in phase r of a solvent. $\Delta\Sigma_1^{(NI)}$ is the transition entropy of a solvent, x_2 is the mole fraction of the solute and μ_2^0 and $\mu_2^{(r)}$ and are, respectively, the chemical potentials of a solute in the pure state and in the mixture under conditions corresponding to $N-I$ transition of component 1.

Expressions for $\gamma_{2,\infty}^{(r)}$ may be obtained from (20), (22) by straightforward means:

$$\begin{aligned}\ln\gamma_{2,\infty}^{(r)} = &-1 - (P_1^*)_{NI}\cdot\frac{v_2}{v_1} + \ln s_{\alpha 2}^{\infty} \\ &+ \ln\left[\frac{\eta_1^{(r)}}{v_1\cdot(1-\eta_1^{(r)})}\right] \\ &+ \frac{\eta_1^{(r)}}{1-\eta_1^{(r)}}\sum_{i=1}^{3}\left(f_{\alpha 2}^{(i)}a_i^{(1)} + \frac{f_2}{f_{\alpha 2}^{(i)}}b_i^{(1)}\right) \\ &+ \frac{(\eta_1^{(r)})^2}{(1-\eta_1^{(r)})^2}\prod_{i=1}^{3}a_i^{(1)}\sum_{i=1}^{3}\frac{f_2}{f_{\alpha 2}^{(i)}}\frac{1}{a_i^{(1)}} - \beta\mu_2^0,\end{aligned} \tag{32}$$

where $s_{\alpha 2}^{\infty}$ is the fraction of solute particles with orientation α, $\eta_1^{(r)}$ is the reduced density of a solvent in the phase r at coexistence and the quantities $a_i^{(1)} \equiv \sum_{\alpha=1}^{6} s_{\alpha 1}/f_{\alpha 1}^{(i)}$ and $b_i^{(1)} \equiv \sum_{\alpha=1}^{6} s_{\alpha 1}f_{\alpha 1}^{(i)}/f_1$ relate to the pure solvent.

Taking into account equations (31), (32) and equation (22) in the form $\mu_2 = \mu_{\alpha 2}$,$(\alpha = 1-3)$, and also following the labelling convention shown in figure 1, one can calculate the fractions $s_{\alpha 2}^{\infty}$ from the following set of equations, which pertain, in general, to biaxial particles:

$$\begin{aligned}&\ln s_{12}^{\infty} + w_{12} = \ln s_{22}^{\infty} + w_{22}, \\ &\ln s_{12}^{\infty} + w_{12} = \ln s_{32}^{\infty} + w_{32} \\ &2\sum_{\alpha=1}^{3} s_{\alpha 2}^{\infty} = 1,\end{aligned} \tag{33}$$

where

$$\begin{aligned}w_{\alpha 2} = &\frac{\eta_1^{(r)}}{1-\eta_1^{(r)}}\sum_{i=1}^{3}\left(f_{\alpha 2}^{(i)}a_i^{(1)} + \frac{f_2}{f_{\alpha 2}^{(i)}}b_i^{(1)}\right) \\ &+ \frac{(\eta_1^{(r)})^2}{(1-\eta_1^{(r)})^2}\prod_{i=1}^{3}a_i^{(1)}\sum_{i=1}^{3}\frac{f_2}{f_{\alpha 2}^{(i)}}\frac{1}{a_i^{(1)}}.\end{aligned}$$

If the z axis is chosen as the director of the uniaxial nematic fluid (see figure 1), then the fractions of rods pointing in the x and y directions are the same. The order parameters of short and long rods in the mixtures are, respectively, $S_{R_1}^0 = -1/2 + 3s_{11}^0$ and $S_{R_2}^{\infty} = -1/2 + 3s_{12}^{\infty}$. In the discotic nematic phase, the normals to the square facets of the plates are predominantly aligned along the director, so the order parameters of the thick and thin platelets are $S_{P_1}^0 = -1/2 + 3s_{31}^0$ and $S_{P_2}^{\infty} = -1/2 + 3s_{32}^{\infty}$. It is noteworthy that the values of $\beta_{2,\infty}^{(r)}$ can be calculated using only data on the transition properties of a pure liquid crystal solvent and the geometrical features of both components. If one permutes the indices corresponding to the components in expressions (30) and (31), one obtains expressions for the co-existence boundaries in the vicinity of a pure second component.

The requirement for a hard core isotropic fluid mixture to be stable with respect to de-mixing is the positive definiteness of the Hessian matrix of the Helmholtz energy density, F/V, as a function of the partial densities ρ_ν [17, 40, 41]:

$$M_{\nu\lambda} \equiv \beta\frac{\partial^2(F/V)}{\partial\rho_\nu\partial\rho_\lambda} = \beta\frac{\partial\mu_\nu}{\partial\rho_\lambda}, \tag{34}$$

where $\mu_\nu = (\partial F/\partial N_\nu)_{N_{\lambda\neq\nu},V} = (\partial(F/V)/\partial\rho_\nu)_{\rho_\lambda}$ is the chemical potential of component ν. This condition reflects the stability of a mixture both with respect to volume and composition fluctuations and can also be regarded as the condition of stability with respect to diffusion at constant pressure [40–42]. Elements of the 2×2 matrix $\hat{M}$ for an isotropic binary cuboid mixture can be analytically computed by using the following expression for F_{conf}/V, obtained from equations (25) and (27):

$$\begin{aligned}\beta\left(\frac{F_{conf}}{V}\right) = &-(\rho_1+\rho_2)(1+\ln 6 + \ln(1-v_1\rho_1 - v_2\rho_2)) \\ &+ \rho_1\ln\rho_1 + \rho_2\ln\rho_2 \\ &+ \frac{1}{24}\frac{(\sigma_1\rho_1+\sigma_2\rho_2)(P_1\rho_1+P_2\rho_2)}{1-v_1\rho_1-v_2\rho_2} \\ &+ \frac{1}{216}\frac{(\sigma_1\rho_1+\sigma_2\rho_2)^3}{(1-v_1\rho_1-v_2\rho_2)^2}\end{aligned}$$

Here, the reduced energy is represented as a function of elementary geometrical features of the particles. In this case these are: the volume v_v, the surface area $\sigma_\kappa = 2(2L_\lambda D_\lambda + D_\lambda^2)$ and the sum of the edges lengths $P_\lambda = 4(L_\lambda + 2D_\lambda)$.

To locate a spinodal curve, it is necessary to solve the equation:

$$\det \hat{M} = 0. \tag{36}$$

For mixtures of cuboidal particles of dimensions $L_i \times D_i \times D_i$ the result is expressed as a function of several variables, i.e. the packing fraction η, the volume fraction of species 1 (φ_1), and the geometrical characteristics Γ_2, $\Gamma = \Gamma_1/\Gamma_2$ and $r = D_1/D_2$. The expression is given in Appendix 3. Expression (A3.1), in the case of a mixture of parallel cubes, reduces to equation (22) in [17], which was derived by use of fundamental measure theory. If there is a solution of equation (36), one finds two values of the volume fraction, φ_1, for a given value η and these correspond to the spinodal boundaries.

3.3. *Results*

Before analysing our results for mixtures, we present data for the order parameters and some thermodynamic properties at the $N-I$ transition for a one-component fluid of rods with $\Gamma_{1R} = 15$ and a one component fluid of plates with $\Gamma_{1P} = 1/15$. The plate values are given in parentheses. The data are: $S_1^0 = 0.83432$ (0.68783), $(P_1^*)_{NI} = 0.21071$ (0.18702), $\eta_N = 0.10760$ (0.09132), $\eta_I = 0.087140$ (0.078945) and $\Delta\Sigma_{NI} = 0.45977$ (0.32102). Reduced values of the coexistence pressures in a fluid of long rods with $\Gamma_{2R} = 150$ and of thin plates with $\Gamma_{2P} = 1/150$ are 0.015914 and 0.014580, respectively. In comparison with hard-particle models with continuous orientations, the numerical values of the $N-I$ transition parameters of the Zwanzig model are substantially smaller while the order parameters are higher. Indeed, for freely rotating hard cylinders with length-to-diameter ratio of 15 one has $S = 0.78$, $P_{NI}^* = 1.304$, $\eta_N = 0.217$, $\eta_I = 0.190$, $\Delta\Sigma_{NI} = 0.854$ [7]. The reason for this difference is the reduction of the orientational entropy due to the restricted number of allowed orientations ([34] and references therein). This effect causes a decrease in the coexistence densities and enhances the orientational order.

Now we proceed to the results relating to $N-I$ phase coexistence in the mixtures under investigation. A common trend in both the R_1-R_2 and P_1-P_2 systems is readily apparent from figure 4. At comparatively small values of d (i.e. at small values of the volume ratio, v_1/v_2), $\beta_{2,\infty}^{(N)} < 0$, so the addition of a thin rod or an extremely thin plate results in the elevation of t^*. Thus, under these conditions mixing stabilizes the nematic phase. For larger values of d (or larger values of v_1/v_2), the reverse is true – $\beta_{2,\infty}^{(r)} > 0$, so mixing destabilises the nematic phase. If the molecular volume of the solvent (component 1) is similar to that of component 2 ($v_1/v_2 < 3$ both for R_1-R_2 and P_1-P_2 mixtures), strong fractionation is observed. This is the situation when the shorter rods and thicker platelets are mostly concentrated in the isotropic phase. Similar results have been reported for mixtures of freely rotating rods [7].

Such an effect is explicitly shown in terms of the distribution constants $K_2^\infty = \lim_{x_2\to 0}(x_2^{(N)}/x_2^{(I)})$ (see inset in figure 4). For a given value of d, however, the stabilization of the nematic phase and the fractionation between coexisting phases are both weaker for plates than for rods. This may result from the fact that plates are less ordered than rods at the $N-I$ transition. Results of the present study, if the values v_1/v_2 of constituent particles are sufficiently small, seem also qualitatively corroborating the data of Harnau and Dietrich [20; (2002)]. They studied inhomogeneous and bulk homogeneous hard-platelet and hard-rod colloidal fluids in the limit of infinite anisometry of particles. It has been shown that in binary bulk mixtures smaller particles concentrate in the isotropic phase. The stability of

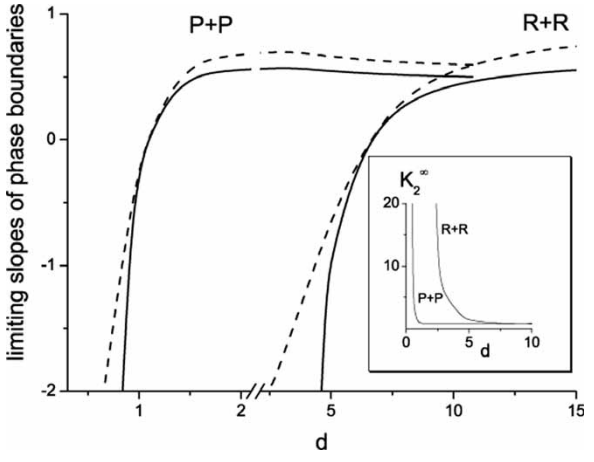

Figure 4. The limiting binodal stability boundaries $\beta_{2,\infty}^{(r)}$ versus $d = D_{1j}/D_{2j}$ ($j = R,P$), the ratio of the cross-sectional sides of the two components. The plots correspond to a dilute solution of component 2 in a solvent of component 1. The solid curves correspond to the isotropic phase while the dashed curves correspond to the nematic. The molecular volumes and aspect ratios are given by: $v_{1R} = v_{1P}$, $v_{2R} = v_{2P} = 150$; and $\Gamma_{1R} = \Gamma_{1P}^{-1} = 15$; $\Gamma_{2R} = \Gamma_{2P}^{-1} = 150$. Inset. For the same binary mixtures, we plot the distribution coefficient of the additive (component 2) at infinite dilution, $K_2^\infty = \lim_{x_2\to 0}(x_2^{(N)}/x_2^{(I)})$, where $x_2^{(r)}$ are mole fractions of component 2 in the coexisting phases ($r = I, N$).

nematic phase and fractionation in composition is manifested weaker in the mixture of vanishingly thin platelet as compared with the corresponding mixture of rods. In the case of thin rods, the results of Harnau and Dietrich are in agreement with earlier calculations [13].

The order parameters $S_{R_2}^{\infty}$ and $S_{P_2}^{\infty}$ of the dissolved long rods and thin plates are presented in figure 5 as functions of the ratio v_1/v_2 (in terms of the ratio d). At large values of v_1/v_2, component 1 corresponds to particles with colloid dimensions. In such situations one can see that the limiting values $S_{R_2}^{\infty}$ and $S_{P_2}^{\infty}$ in the solution are significantly smaller than their values in the pure fluids at the I–N transition. These values are 0.9060 and 0.8109, respectively. Owing to a huge difference in molecular volumes a polymeric rod orders quite weakly in the nematic matrix of the first component, at least for low polymer concentrations. Similar phenomena are observed in the mixtures of freely rotating rods with aspect ratios 15 and 150 when they have very large differences in volume [7].

As well as undergoing isotropic–nematic transitions, hard-rod and hard-platelet blends may exhibit both $I-I$ and $N-N$ de-mixing. These issues have been explored in a large number of simulation and theoretical studies. Although the results of these studies turn out to be sensitive to the fine details of the model and the precise nature of the theory used [43], they indicate that the phase diagrams of binary mixtures of anisometric particles are very sensitive to the choice of molecular parameters, i.e. to the aspect ratios of particles and their size ratios.

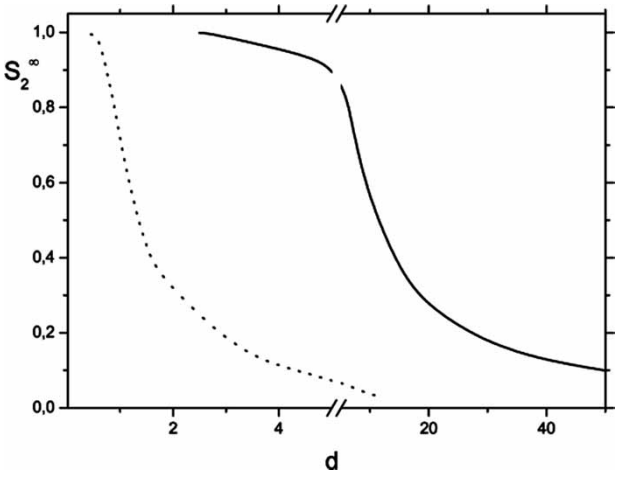

Figure 5. The order parameter of the second component at infinite dilution versus the ratio of cross-sectional sides of the components d. The solid line is for the $R-R$ mixture and the dashed line for the $P-P$ mixture. The definition d and the values of the molecular parameters are as in figure 4.

It should be noted that FMT studies on binary mixtures of square platelets with restricted orientations [19, 20] suggest the possibility of $N-N$ demixing for certain size and width ratios. No such $N-N$ de-mixing, however, has been reported in the corresponding rod mixtures [44]. The question of this type phase split as it makes appearance in the present variant of the Zwanzig model in application to mixtures of rods different in aspect ratios and volumes is being currently investigated.

We now consider our results for $I-I$ de-mixing in the R_1-R_2 and P_1-P_2 systems. Figure 6 shows the density-composition diagrams for de-mixing instabilities for two binary rod mixtures (1R and 2R) and two binary plate mixtures (1P and 2P). As before, the aspect ratios of the rods are the inverses of those of the plates whilst we have set $v_1/v_2=2700$ for 1R and 1P and $v_1/v_2=6400$ for 2R and 2P. Also shown is a spinodal curve for a mixture of parallel cubes with $v_1/v_2=6400$. The results show that the regions of the phase diagram corresponding to unstable states are strongly dependent upon the shape of the particles of both components. Qualitatively the difference is due to the fact that platelet mixtures are stable with respect to de-mixing up to extremely high densities, while rod-like mixtures with similar size ratios may demix even at very low values of η.

In figure 7, we plot the consolute density against v_1/v_2 for a binary rod and a binary plate mixture (parameters the same as those given in figure 4). Compared with the rods, demixing in the platelet mixture only sets in at very

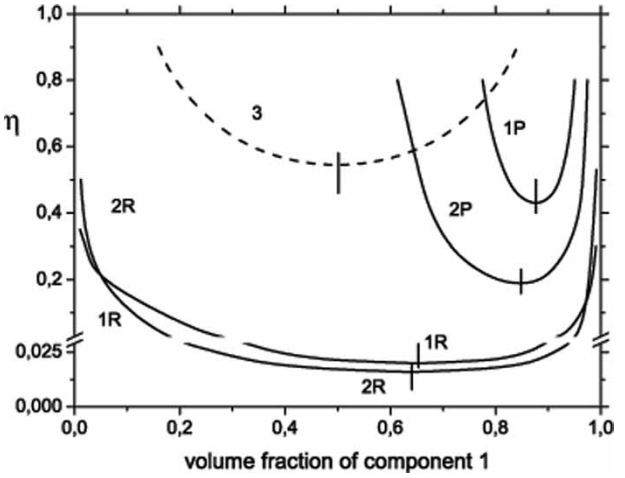

Figure 6. Spinodal densities corresponding to $I-I$ demixing for rods (R) and plates (P), for mixtures of rectangular hard cuboids. The values of the molecular parameters are as in figure 4. The mixtures are: $v_1/v_2=2700$ (1): $d=30$ (R) and 6.4633 (P); $v_1/v_2=6400$ (2); $d=40$ (R) and 8.6177 (P). The dashed curve (3) corresponds to a mixture of parallel cubes $v_1/v_2=6400$ ($d=18.56635$). Vertical lines show the location of consulute points.

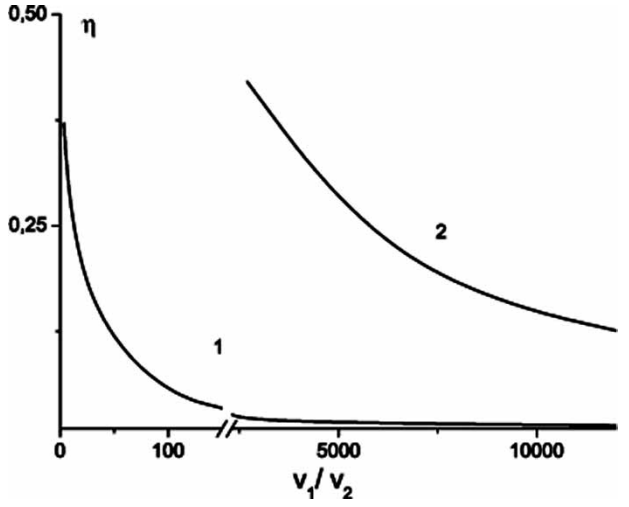

Figure 7. Densities at the consolute points for corresponding rod and plate mixtures. The values of the molecular parameters are as in figure 4.

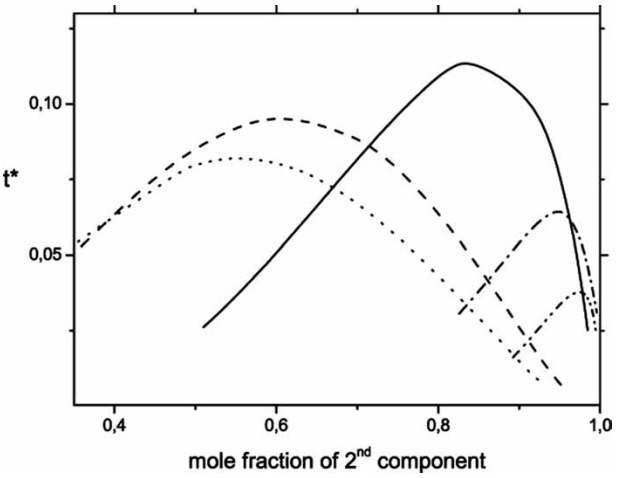

Figure 8. Spinodal curves corresponding to $I-I$ de-mixing in binary rod mixtures R_1-R_2 with the dimensions of the second component particles fixed at $150\times1\times1$. The legend corresponding to various dimensions of the first component particles: solid line – $150\times10\times10$; dashes – $75\times5\times5$; dots – $(4.5\times15)\times4.5^2$; dashes-dotted curve – $300\times20\times20$; dash-dot-dotted curve – $450\times30\times30$.

high values of v_1/v_2 and at considerably higher overall densities. Indeed for $v_1/v_2=1690$, the consolute packing fraction for plates is predicted to be approximately 0.95. In reality, of course, one would expect a phase transition to ordered states to occur long before this demixing instability. For comparison we note that in the parallel cube mixture, demixing occurs when the volume of the large species is approximately 1000 times greater than that of the smaller one [17].

Figure 8 plots $I-I$ spinodals for a number of R_1-R_2 blends, using as variables t^* and composition. The positions of the I–I domains in cuboid mixtures viewed show similarities to those found in mixtures of freely rotating cylinders, calculated by a functional scaling method (figures 1, 2(e) and 3(a) in [7]). Increasing the diameter ratio of the species results in an expansion of these domains. A noticeable feature is that the compositions of the consolute points calculated here coincide very closely those obtained for bi-disperse mixtures of freely rotating cylinders, for similar geometric parameters of the species [7]. Unlike the freely rotating rods, however, $I-I$ de-mixing in our model is meta-stable with respect to a $N-I$ transition for all of the binary mixtures studied. Figure 9(a) may illustrate the consequence of orientational discretization for a system with colloidal component $150\times10\times10(d_R=10)$: the reduced temperature of the $I-I$ consolute point ($t^*\cong0.11$; see figure 8) is below the domain of $N-I$ coexistence. Similar observations apply to the whole of the R_1-R_2 series with our chosen set of aspect ratios ($\Gamma_2=150$, $\Gamma_1=15$) where the reduced temperature of the $N-I$ transition of the pure second component is given by $t^*=13.2407\times(v_{2R}/v_{1R})$. It can be directly checked that the temperatures of the consolute points shown in figure 8 never surpass the upper boundary of the $N-I$ equilibrium domain.

The R_1-R_2 mixtures in the present model exhibit certain features of the phase diagram which have much in common with blends of freely rotating components with the same d_R. Figure 9(b), relating to a mixture with $d_R=4.5$, illustrates this. Apart from the fact that $I-I$ de-mixing turns out to be meta-stable with respect to nematic phase formation in both approaches, one comes across a manifestation of an azeotrope in the $N-I$ coexistence domain, its composition being very close to that given in [7]. The infinite dilution tangents of the nematic and isotropic phase boundaries of figure 9(b) are also virtually the same as in [7].

The results obtained are in line with general trends in binary mixtures of hard convex bodies, observed in the frame of the scaled particle approximation [43]: fluid–fluid phase separation can result from substantial asymmetries between the breadths of molecular species. In the context of these studies it is significant that recent theoretical methods based on the FMT in the Zwanzig approximation and the modified Onsager theory ([18]; (2004); [45], and references therein) show that fluids of anisotropic particles tend to form different bulk inhomogeneous phases (such as smectic, columnar or solid) at moderate and high packing fractions. Thus, the $I-I$ and $N-I$ separation may be metastable with respect to apparition of regions where smectic phases of different structure and composition coexist.

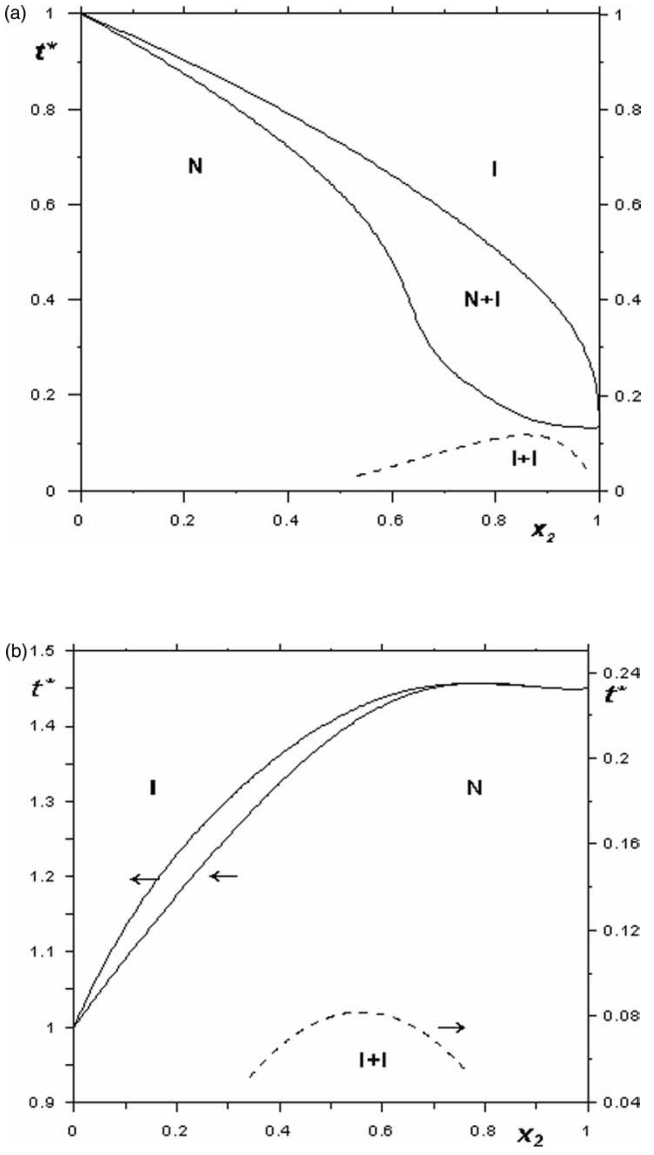

Figure 9. Equilibria involving isotropic and nematic phases in two blends of rods with linear dimensions: (a) $150 \times 10 \times 10$ and $150 \times 1 \times 1$; (b) $67.5 \times 4.5 \times 4.5$ and $150 \times 1 \times 1$.

However, the model under consideration is not suited to the description of spatially inhomogeneous phases of biaxial particles, so, in this paper we address the study of $I-I$ de-mixing and $N-I$ transitions and comparison with the recent results obtained in work [7] from the Onsager model in the Parsons–Lee approximation.

Although our theory includes the effects of triplet correlations, we now see whether we can qualitatively understand our demixing results in terms of the large, unfavourable excluded volume interactions between unlike species [46].

The mixed excluded volume in the isotropic binary HRP solution takes the form:

$$V_{excl}^{(iso)} = \frac{1}{3}(D_1 + D_2)^2 \cdot (L_1 + L_2) + \frac{2}{3}(D_1 + D_2) \cdot (D_1 + L_2) \cdot (D_2 + L_1), \quad (37)$$

where the terms on the r.h.s. relate to contributions coming from the parallel and orthogonal orientations of two square cuboids of species 1 and 2, accordingly. The formula applies both to the mixtures of rods and plates. The calculated reduced orientation-averaged excluded volumes in corresponding binary $R_1 - R_2$ and $P_1 - P_2$ mixtures, $\tilde{V}_{\text{excl}}^{(\text{iso})} = V_{\text{excl}}^{(\text{iso})}/V_{\text{cube}}$, are given below ($V_{cube} = (\Gamma_1^{1/3} D_1 + \Gamma_2^{1/3} D_2)^3$ is the excluded volume of an one-component fluid of cubes with molecular volume arithmetic-averaged between the volumes of cuboids of the binary mixture):

v_1	d_R	$\tilde{V}_{\text{excl}}^{(\text{iso})}$ for rods	$\tilde{V}_{\text{excl}}^{(\text{iso})}$ for plates
1875000	50	2,767	1,891
120000	20	4,780	3,093
50625	15	5,676	3,693
3240	6	8,627	6,417
405	3	9,643	8,681
234.375	2.5	9,564	9,119

The molecular parameters for the mixtures are the same as described above.

Inspection of the above data shows that the excluded volumes in the $R_1 - R_2$ blends are systematically greater than in the $P_1 - P_2$ mixtures. Demixing is thus favoured in the rod mixture, in agreement with the results of our full calculations (figures 6 and 7).

An estimate of critical platelet aspect ratios necessary for depletion-induced de-mixing of homogeneous nematic phases has been obtained recently in the study [19] within the second virial approximation of the excess free energy. Concrete estimates have been given for completely ordered nematic phases. The criterion obtained therein can be also applied in the analysis of *I–I* de-mixing. Thus, to some extent simple estimates based on equation (35) may complement the results of the work [19].

4. Conclusions

This work and the preceding ones [29, 30] present generalizations of the Flory–DiMarzio probabilistic scheme of calculating excess Helmholtz energy in the

case of multi-component systems of hard biaxial parallelepipeds with restricted sets of orientations. On taking the limit of zero-lattice spacing, the EOS coincides with that obtained by a variety of different theoretical approaches, making seemingly quite unrelated approximations. Examples are the complete star approximation [36], the third level y-expansion [21] and a fundamental-measure theory [18, 19] for homogeneous phases. We also compared several predictions of our aproach with previous studies on mixtures of freely rotating particles [7]. Similar trends were observed, again suggesting that this model is capable of capturing the essential physics of the phase behaviour of binary mixture of hard anisometric particles, at least for translationally disordered phases.

A complete theoretical investigation into the phase behaviour of fluids with mesogenic components would require the study of the stabilities of translationally ordered phases as well as the isotropic and nematic phases considered here. In the case of systems containing axially symmetric particles, fundamental measure theory in the Zwanzig approximation has been successfully used to treat smectic and columnar phases [18, 20, 45], bulk properties and free interfaces in fluids of charged plate-like colloids [47].

The presence of molecular bi-axiality would no doubt generate still richer phase behavior with a complex interplay of phase stabilities in mixtures. We believe that the model presented here could be useful for studying uniaxial and biaxial nematic stability in this kind of systems. Another matter of interest for physico-chemical application is to consider the attraction between bi-axial particles by a suitable generalization of a square-well model for uniaxial particles, in spirit to the study [32] proposed recently.

Acknowledgements

We acknowledge the support of the Royal Society, UK, in providing a travel grant which made this collaboration possible. EPS and AYV were supported by the Foundation 'Science Schools of Russian Federation' (grant NS-5557.2006.3). The authors would also like to thank Dr A. N. Marinichev for his generous assistance with the calculations.

Appendix 1

Equation (15) has also been derived for hard parallel cubes by noting that each virial coefficients, up to order 7, is approximately equal to the complete star integral multiplied by the corresponding Ree–Hoover weight [37]. Mitra and Allnatt [36] in a study of defects in the crystal UO_{2+x} used this approximation to estimate the equation of state of a lattice gas of rectangular parallelepipeds. This approximation yields an equation of state which is necessarily exact up to the third virial.

By retaining solely the contributions of complete-star integrals, one is in a position to analytically calculate the excess entropy of a multi-component lattice gas of hard cuboids. For these systems, the Mayer-f function is a product of three, one dimensional Mayer functions, corresponding to the interaction of hard rods along the x, y and z axes of the lattice. The complete star integrals thus become a product of three hard rod star integrals, where the hard rod star corresponds to a mixture of one dimensional hard rods. In the one-dimensional case, Mitra and Allnatt obtained an analytical expression for the hard rod complete star integral of any order. This enabled them to calculate the complete star for the hard cuboids and hence allow an estimate of all the virial coefficient. It proved possible to sum this series analytically to give, in the notation of section 2:

$$\frac{\Sigma_c}{k_B M} = -\sum_{n=1}^{8} g^{(n)}\left\{\left(1-h^{(n)}\right)\ln\left(1-h^{(n)}\right)+h^{(n)}\right\} + \sum_{\lambda=1}^{6k}\left(\frac{N_\lambda}{M}\right)\ln\left(\frac{N_\lambda}{Me}\right). \tag{A1.1}$$

Here, k stands for a number of components, whilst the rest of the quantities on the r.h.s. are:

$$g^{(1)} = -g^{(2)} = -g^{(3)} = -g^{(4)} = g^{(5)} = g^{(6)} = g^{(7)} = g^{(8)} = 1,$$

$$h^{(n)} = \sum_{\lambda=1}^{6k}\frac{f_\lambda^{(n)} N_\lambda}{M}$$

$$f_\lambda^{(1)} = r_\lambda,\ f_\lambda^{(4)} = r_\lambda\left(1-\frac{1}{r_\lambda^{(3)}}\right),$$

$$f_\lambda^{(2)} = r_\lambda\left(1-\frac{1}{r_\lambda^{(1)}}\right),\ f_\lambda^{(5)} = r_\lambda\left(1-\frac{1}{r_\lambda^{(1)}}\right)\left(1-\frac{1}{r_\lambda^{(2)}}\right),$$

$$f_\lambda^{(3)} = r_\lambda\left(1-\frac{1}{r_\lambda^{(2)}}\right),\ f_\lambda^{(6)} = r_\lambda\left(1-\frac{1}{r_\lambda^{(1)}}\right)\left(1-\frac{1}{r_\lambda^{(3)}}\right),$$

$$f_\lambda^{(7)} = r_\lambda\left(1-\frac{1}{r_\lambda^{(2)}}\right)\left(1-\frac{1}{r_\lambda^{(3)}}\right),\ f_\lambda^{(8)} = \prod_{i=1}^{3}\left(r_\lambda^{(i)}-1\right).$$

With some further algebra one may confirm the equivalence of formulae (A1.1) and (15).

Table A2. Dependence of the virial coefficients for a system of parallel cubes on the mesh size (the exact values are denoted with asterisk).

W	B_2	B_3	B_4	B_5	B_6
2	1.69	1.79	1.65	1.45	1.27
2*	1.69	1.79	1.35	0.73	0.17
3	2.32	3.14	3.49	3.54	3.42
4	2.68	4.12	5.11	5.68	5.92
5	2.92	4.84	6.43	7.60	8.37
∞	4	9	16	25	36
∞*	4	9	11.33	3.16	−18.88

Appendix 2

One may use equations (16) and (21) to calculate virial coefficients as given by our approximate theory. For the parallel cube fluid, we find that for the lattice gas we have $B_n^{(latt)} = w^3[1-(1-1/w)^n]^3/n$ while in the translationally continuous limit we have $B_n = \lim_{w\to\infty} B_n^{(latt)} = n^2$, where $w^3\Delta v = v$ is the volume of a cube occupying w^3 lattice cells. In table A2, the first 5 virial coefficients (in units of a particle volume) are compared with the exact values given in [37].

As may be seen, both the lattice and the continuum versions of the model are exact up to the third virial coefficient. Reducing the mesh size causes all the virial coefficients to decrease. This shows that the presence of a lattice reduces the strength of steric interactions. The radius of convergence of the lattice virial series may be significantly different from that of the continuum series. The behaviour 'of the model fluid' observed at the high density in the 'lattice gas treatment' may differ qualitatively, as well as quantitatively, from that of its continuum analogue [37]. These effects must be borne in mind when using lattice models to study ordered phases, such as the smectic A phase.

Appendix 3

Straightforward though lengthy calculations of $\det\hat{M}$ can be readily carried out with any symbol algebra system. Using equations (31, 32) one can obtain:

$$\rho_1\rho_2 \det\hat{M} = \frac{64\eta^2}{(1-\eta)^4}\left[\frac{F_0}{\eta^2}+\frac{F_1}{\eta}+F_2\right], \qquad \text{(A3.1)}$$

where

$$F_0 = 9r\Gamma^2\cdot\Gamma_2^2,\ F_1 = F_{10}+\varphi_1 F_{11},$$

$$F_2 = F_{20}+\varphi_1 F_{21}+\varphi_1^2 F_{22},$$

$$F_{10} = 12r\Gamma^2\cdot\Gamma_2\cdot(1+\Gamma_2+\Gamma_2^2),$$

$$F_{11} = 12r\Gamma\cdot\Gamma_2\cdot(\Gamma-1)(\Gamma\cdot\Gamma_2^2-1),$$

$$F_{20} = r\Gamma^2\cdot(2+3\Gamma_2^2+4\Gamma_2^3),$$

$$F_{21} = -(t_1\Gamma+t_2\Gamma^3)+r(-t_3\Gamma+t_4\Gamma^2-t_3\Gamma_2^2\Gamma^3)-r^2t_5$$

$$F_{22} = (t_1\Gamma+t_2\Gamma^3)+r(2+t_3\Gamma+t_6\Gamma^2+t_7\Gamma^3)+r^2t_5$$

$$t_1 = 2(1+2\Gamma_2)^2,\ t_2 = t_1\Gamma_2^2/2,$$

$$t_3 = -8(1+\Gamma_2+\Gamma_2^2),\ t_4 = -2(2-4\Gamma_2-\Gamma_2^2)$$

$$t_5 = \Gamma\cdot(2+\Gamma_2^2)(1+2\Gamma\cdot\Gamma_2)^2,$$

$$t_6 = -2(-1+4\Gamma_2+\Gamma_2^2+2\Gamma_2^3),$$

$$t_7 = -4\Gamma_2^2(2+\Gamma_2+2\Gamma_2^2).$$

In the particular case of a mixture of parallel hard cubes ($\Gamma=\Gamma_2=1$), except for an irrelevant factor $576r$, expression (A3-1) reduces to the result obtained by Cuesta in the frame of FMT [17]:

$$\rho_1\rho_2 \det\hat{M} = \frac{576r\eta^2}{(1-\eta)^4}\left[1+\frac{4}{\eta}+\frac{1}{\eta^2} - 3\varphi_1(1-\varphi_1)\frac{(r-1)^2}{r}\right] \qquad \text{(A3.2)}$$

References

[1] G. J. Vroege and H. N. W. Lekkerkerker, Phil. Trans. R. Soc. Lond. A. **344,** 419 (1993).
[2] T. M. Birshtein, B. I. Kolegov, and V. A. Pryamitsyn, Polym. Sci. USSR **30,** 316 (1988).
[3] R. van Roji, B. Mulder, and M. Dijkstra, Physica A **261,** 374 (1998).
[4] P. C. Hemmer and T. H. Marthinsen, Mol. Phys. **100,** 667 (2002).
[5] L. Onsager, Ann. N. Y. Acad. Sci. **51,** 627 (1949).
[6] S. D. Lee, J. Chem. Phys. **87,** 4972 (1987).
[7] S. Varga, A. Galindo, and G. Jackson, Mol. Phys. **101,** 817 (2003).
[8] P. J. Camp, and M. P. Allen, Physica A **229,** 410 (1996); H. H. Wensink, G. J. Vroege, and H. N. W. Lekkerkerker, J. Chem. Phys. **115,** 7319 (2001); S. Varga, A. Galindo, and G. Jackson, J. Chem. Phys. **117,** 7207 (2002).
[9] H. H. Wensink, G. J. Vroege, and H. N. W. Lekkerkerker, J. Phys. Chem. B **105,** 10610 (2001).
[10] M. P. B. van Bruggen, F. M. van der Kooij, and H. N. W. Lekkerkerker, J. Phys.: Condens. Matter **8,** 9451 (1996).

[11] F. M. van der Kooij, D. van der Beek, and H. N. W. Lekkerkerker, J. Phys. Chem. B **105,** 1696 (2001); F. M. van der Kooij, and H. N. W. Lekkerkerker, Phys. Rev. Lett. **84,** 781 (2000).
[12] R. Zwanzig, J. Chem. Phys. **39,** 1714 (1963).
[13] N. Clarke and T. C. B. McLeish, J. Physique II **2,** 1841 (1992).
[14] R. van Roji and B. Mulder, J. Physique II **4,** 1762 (1994).
[15] P. R. Sear and G. Jackson, J. Chem. Phys. **103,** 8684 (1995).
[16] Y. Rosenfeld, J. Chem. Phys. **89,** 4271 (1988).
[17] J. A. Cuesta, Phys. Rev. Lett. **76,** 3742 (1996).
[18] Y. Martínez-Ratón, and J. A. Cuesta, J. Chem. Phys. **118,** 10164 (2003); (2002), Phys. Rev. Lett. **89,** 185701; Y. Martínez-Ratón, Phys. Rev. E **69,** 061712 (2004).
[19] L. Harnau, D. Rowan, and J.-P. Hansen, J. Chem. Phys. **117,** 11359 (2002).
[20] L. Harnau, and S. Dietrich, Phys. Rev. E **66,** 051702 (2002); M. Bier, L. Harnau, and S. Dietrich, Phys. Rev. E **69,** 021506 (2004).
[21] B. Barboy and W. M. Gelbart, J. Stat. Phys. **22,** 685, 709 (1980).
[22] P. J. Flory, Proc. Roy. Soc. (L) **A234,** 73 (1956); A. R. E. Miller, *The Theory of Solutions of High Polymers* (Clarendon Press, Oxford, 1948).
[23] E. A. DiMarzio, J. Chem. Phys. **35,** 658 (1961).
[24] F. Dowell, and D. E. Martire, J. Chem. Phys. **68,** 1088 (1978); F. Dowell, Phys. Rev. A. **28,** 3520, 3526 (1983).
[25] L. Petrone and M. A. Cotter, Phys. Rev. A **40,** 6021, 6045 (1989).
[26] C.-S. Shih, and R. Alben, J. Chem. Phys. **57,** 3055 (1972); R. Alben, J. Chem. Phys. **59,** 4299 (1973).
[27] E. A. DiMarzio, A. J.-M. Yang, and S. C. Glotzer, Res. Nat. Inst. Stand. Technol. **100,** 173 (1995).
[28] R. E. Boehm and D. E. Martire, Liq. Cryst. **12,** 273 (1992).
[29] E. P. Sokolova and N. P. Tumanyan, Liq. Cryst. **27,** 813 (2000).
[30] N. P. Tumanyan, and A. G. Shakhatuni, Armenian Chem. J. **35,** 103 (1982) (in Russian); N. P. Tumanyan, and E. P. Sokolova, Zh. Fiz. Khim. **58,** 2444 (1984) (in Russian).
[31] E. Sokolova, and A. Vlasov, J. Phys.: Condens. Matter **9,** 4089 (1997); E. Sokolova, and A. Vlasov, Fluid Phase Equil. **150–151,** 403 (1998); E. P. Sokolova, I. K. Tochadze, and N. A. Smirnova, Russ. J. Phys. Chem. **75,** 1319 (2001).
[32] E. P. Sokolova, N. A. Smirnova, and I. K. Tochadze, Russ. J. Phys. Chem. **74,** S357 (2000).
[33] M. G. Moore, W. E. McMullen, J. Phys. Chem. **96,** 3374 (1992); J. Chem. Phys. **97,** 9267 (1992).
[34] R. van Roji, M. Dijkstra, and R. Evans, J. Chem. Phys. **113,** 7689 (2000).
[35] S. Singh, Phys. Rep. **324,** 107 (2000).
[36] S. K. Mitra and A. R. Allnatt, J. Phys. C, Solid State Phys. **12,** 2261 (1979).
[37] F. H. Ree, and W. G. Hoover, J. Chem. Phys., **40,** 939 (1964); W. G. Hoover, and A. G. De Rocco, J. Chem. Phys. **36,** 3141 (1962).
[38] R. P. Sear, Mol. Phys. **88,** 1427 (1996).
[39] J. A. C. Veerman, and D. Frenkel, Phys. Rev. A **45,** 5632 (1992); D. Frenkel, J. Phys. Chem. **91,** 4912 (1987).
[40] M. Dijkstra and R. van Roji, Phys. Rev. E **56,** 5594 (1997).
[41] I. Prigogine and R. Defay, *Chemical Thermodynamics* (Longmans Green and Co., 1954).
[42] J. L. Lebowitz, and J. S. Rowlinson, J. Chem. Phys. **41,** 133 (1964). R. van Roji, and B. Mulder, Phys. Rev. E **54,** 6430 (1996).
[43] A. Perera, J. Mol. Liq. **109,** 75 (2004).
[44] P. Sollich, J. Phys.: Condens. Matter **14,** R79 (2002).
[45] Y. Martínez-Ratón, E. Velasco, and L. Mederos, J. Chem. Phys. **123,** 104906 (2005).
[46] S. Varga, A. Galindo, and G. Jackson, Phys. Rev. E **66,** 011707 (2002).
[47] M. Bier, L. Harnau, and S. Dietrich, J. Chem. Phys. **123,** 114906 (2005).